Electronic Supplementary Material (ESI) for Journal of Materials Chemistry A.

Sequence-Dependent Self-Assembly of Supramolecular Nanofibers in Periodic Dynamic Block Copolymers

Jason K. Phong[1†], Christopher B. Cooper[2*†], Lukas Michalek[2], Yangju Lin[2], Yuya Nishio[2], Yuran Shi[2], Huaxin Gong[2], Julian Vigil[2], Jan Ilavsky[3], Ivan Kuzmenko[3], Zhenan Bao[2*].

[1]Department of Materials Science Engineering, Stanford University, Stanford, CA 94305.
[2]Department of Chemical Engineering, Stanford University, Stanford, CA 94305.
[3]Advanced Photon Source, Argonne National Laboratory, Lemont, IL 60439.

[†]Equal Contribution
*Corresponding authors: cbcooper@wustl.edu; zbao@stanford.edu

Table of Contents

Note S1. Derivation of random coil lengths of PEG and PDMS chains

In an ideal Gaussian polymer chain, the average end-to-end distance or the random coil length d is given by:

$$d = b\sqrt{N} \tag{S1}$$

where N is the number of Kuhn monomers and b is the Kuhn monomer length.

For polyethylene glycol (PEG), the Kuhn length is $b_{PEG} = 11$ Å, and the molar mass of the Kuhn monomer is $M_0 = 137\ g\ mol^{-1}$.[1] Therefore, for a PEG chain with a molecular weight of 0.6 kDa, there are ~4.4 Kuhn monomers, giving a random coil length of 23 Å. For a 0.9 kDa PEG chain, there are ~6.6 Kuhn monomers, giving a random coil length of 28 Å.

For polydimethylsiloxane (PDMS), the Kuhn length is $b_{PDMS} = 13$ Å, and the molar mass of the Kuhn monomer is $M_0 = 381\ g\ mol^{-1}$.[1] Thus, for a PDMS chain with a molecular weight of 3 kDa, there are ~7.9 Kuhn monomers, giving a random coil length of 36 Å.

Note S2. Derivation of effective length ratio from ionic conductivity data

Here we map the ionic conductivity observed in the periodic and random DBCPs (σ_{tot}) to ion diffusion through two 1D slabs in series of PEG with length d_{PEG}, and of PDMS with length d_{PDMS}, where the ionic conductivities in each slab is given by σ_{PEG} and σ_{PDMS}, for the PEG and PDMS slabs, respectively. Then the total resistance is given by:

$$R_{tot} = R_{PEG} + R_{PDMS} \tag{S2}$$

$$\frac{d_{tot}}{\sigma_{tot}A} = \frac{d_{PEG}}{\sigma_{PEG}A} + \frac{d_{PDMS}}{\sigma_{PDMS}A} \tag{S3}$$

We note that the resistance is summed in series since the ion travels through the PEG domain and then the PDMS domain of the theoretical 1D slab. We define x as the length of the PDMS slab relative to the total length of both slides, given by $x = \frac{d_{PDMS}}{d_{tot}}$, so that $1 - x = \frac{d_{PEG}}{d_{tot}}$. Then we can write:

$$\frac{1}{\sigma_{tot}} = \frac{1-x}{\sigma_{PEG}} + \frac{x}{\sigma_{PDMS}} \tag{S4}$$

Solving for x we obtain:

$$x = \frac{\sigma_{tot}^{-1} - \sigma_{PEG}^{-1}}{\sigma_{PDMS}^{-1} - \sigma_{PEG}^{-1}} \tag{S5}$$

Finally, we define y as the ratio of PDMS length to PEG length, given by:

$$y = \frac{d_{PDMS}}{d_{PEG}} = \frac{x}{1-x} = \frac{\sigma_{tot}^{-1} - \sigma_{PEG}^{-1}}{\sigma_{PDMS}^{-1} - \sigma_{tot}^{-1}} \tag{S6}$$

We note that the interpretation of y is the effective length ratio of slabs of PDMS and PEG that result in identical bulk conductivity (σ_{tot}) to that measured in the random and periodic DBCPs.

Note S3. Derivation of aspect ratio from a constant shell thickness

Consider a rectangular channel of PEG with width and thickness given by w_{PEG} and length L_{PEG} surrounded by a PDMS shell of uniform thickness d. Then the total volume, volume of PEG and volume of PDMS are given by:

$$V_{tot} = (l_{PEG} + 2d)(w_{PEG} + 2d)^2 \tag{S7}$$

$$V_{PEG} = l_{PEG}{w_{PEG}}^2 \tag{S8}$$

$$V_{PDMS} = V_{tot} - V_{PEG} \tag{S9}$$

Solving for the volume fraction of PEG, we obtain:

$$\frac{1}{\phi_{PEG}} = \frac{V_{tot}}{V_{PEG}} = 1 + 4\frac{d}{w_{PEG}} + 4\frac{d^2}{w_{PEG}^2} + 2\frac{d}{l_{PEG}} + 8\frac{d^2}{w_{PEG}l_{PEG}} + 8\frac{d^3}{w_{PEG}^2 l_{PEG}} \tag{S11}$$

Let a be the aspect ratio of PEG defined by, $a = \frac{l_{PEG}}{w_{PEG}}$. Let y be the length of PDMS relative to the length of PEG along the channel length given by $y = \frac{2d}{l_{PEG}}$. Then by substituting and factoring, we can write:

$$\frac{1}{\phi_{PEG}} = (ay + 1)^2(y + 1) \tag{S12}$$

Finally, solving for the aspect ratio we obtain:

$$a = \frac{1}{y}\left[\left(\frac{1}{\phi_{PEG}(y+1)}\right)^{1/2} - 1\right] \tag{S13}$$

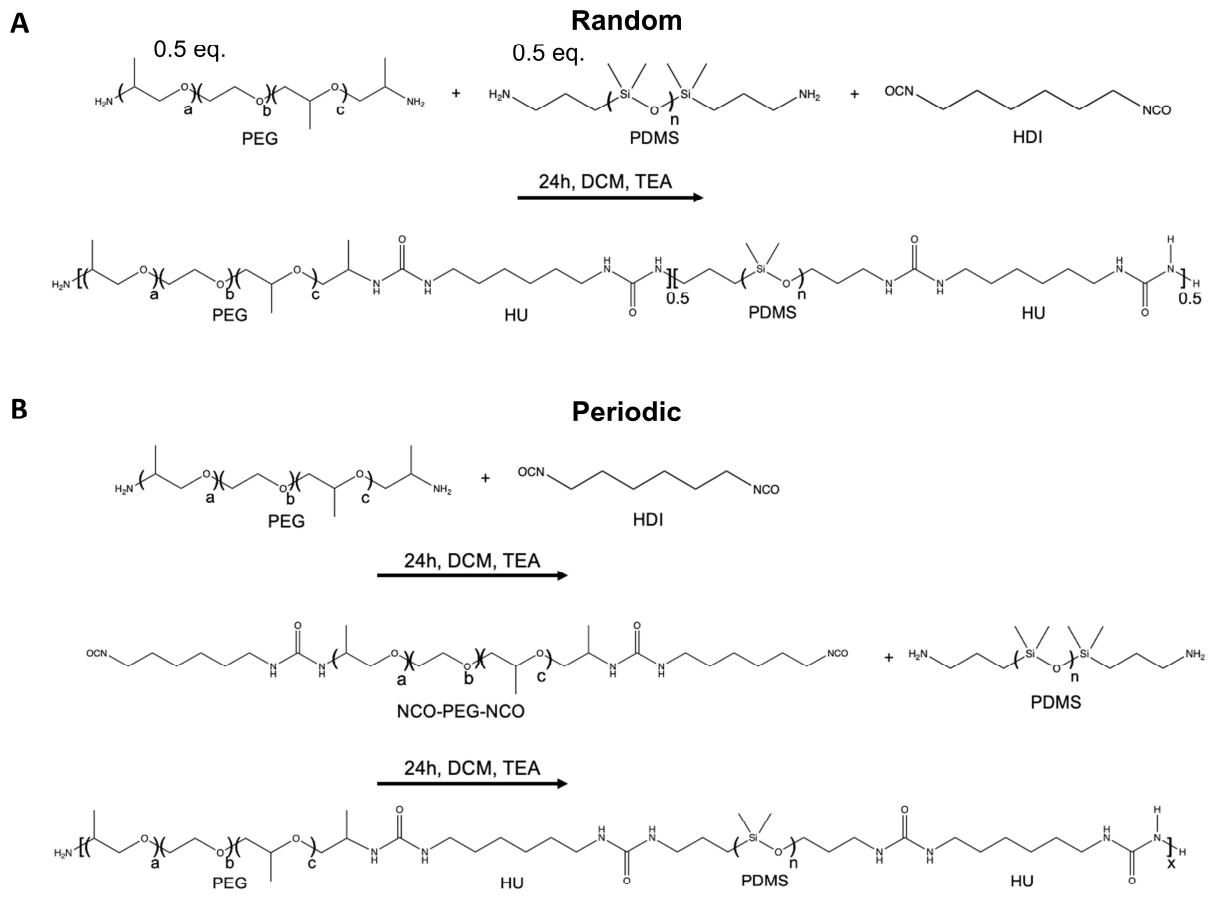

Figure S1. Synthetic routes for **(A)** random and **(B)** periodic DBCPs.

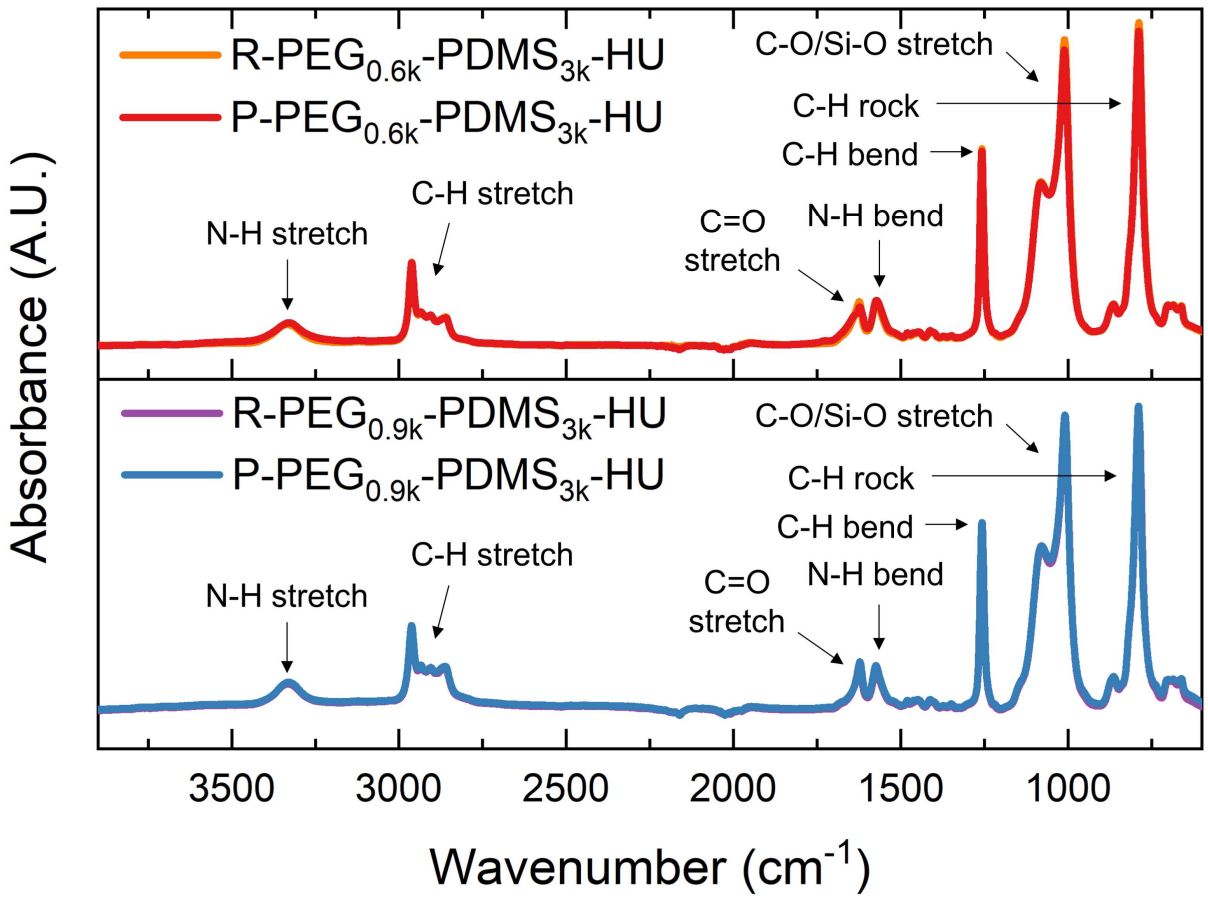

Figure S2. Superimposed FTIR spectra of *R-PEG$_{0.6k}$-PDMS$_{3k}$-HU* (orange) and *P-PEG$_{0.6k}$-PDMS$_{3k}$-HU* (red), and of *R-PEG$_{0.9k}$-PDMS$_{3k}$-HU* (purple) and *P-PEG$_{0.9k}$-PDMS$_{3k}$-HU* (blue).

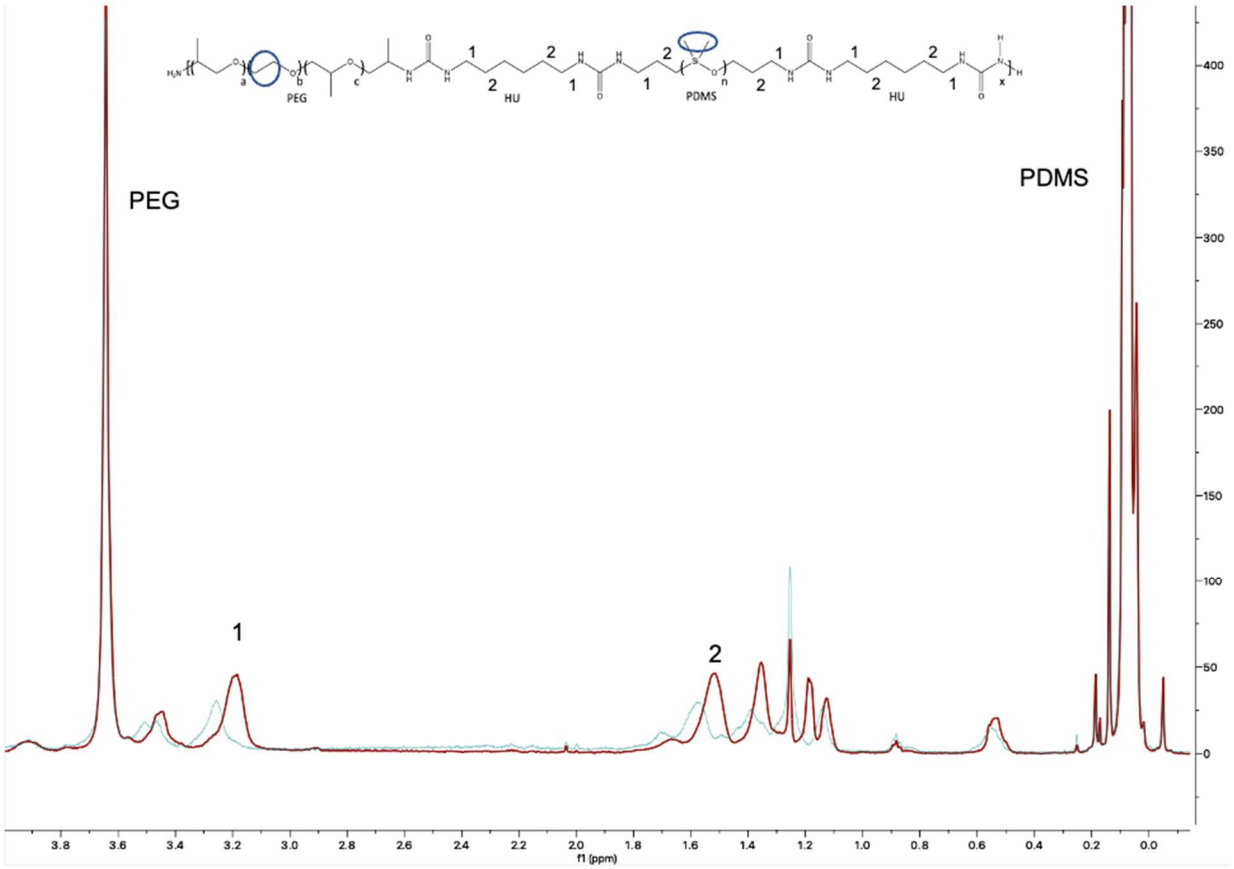

Figure S3. Superimposed NMR spectra of *R-PEG$_{0.6k}$-PDMS$_{3k}$-HU* and *P-PEG$_{0.6k}$-PDMS$_{3k}$-HU*.

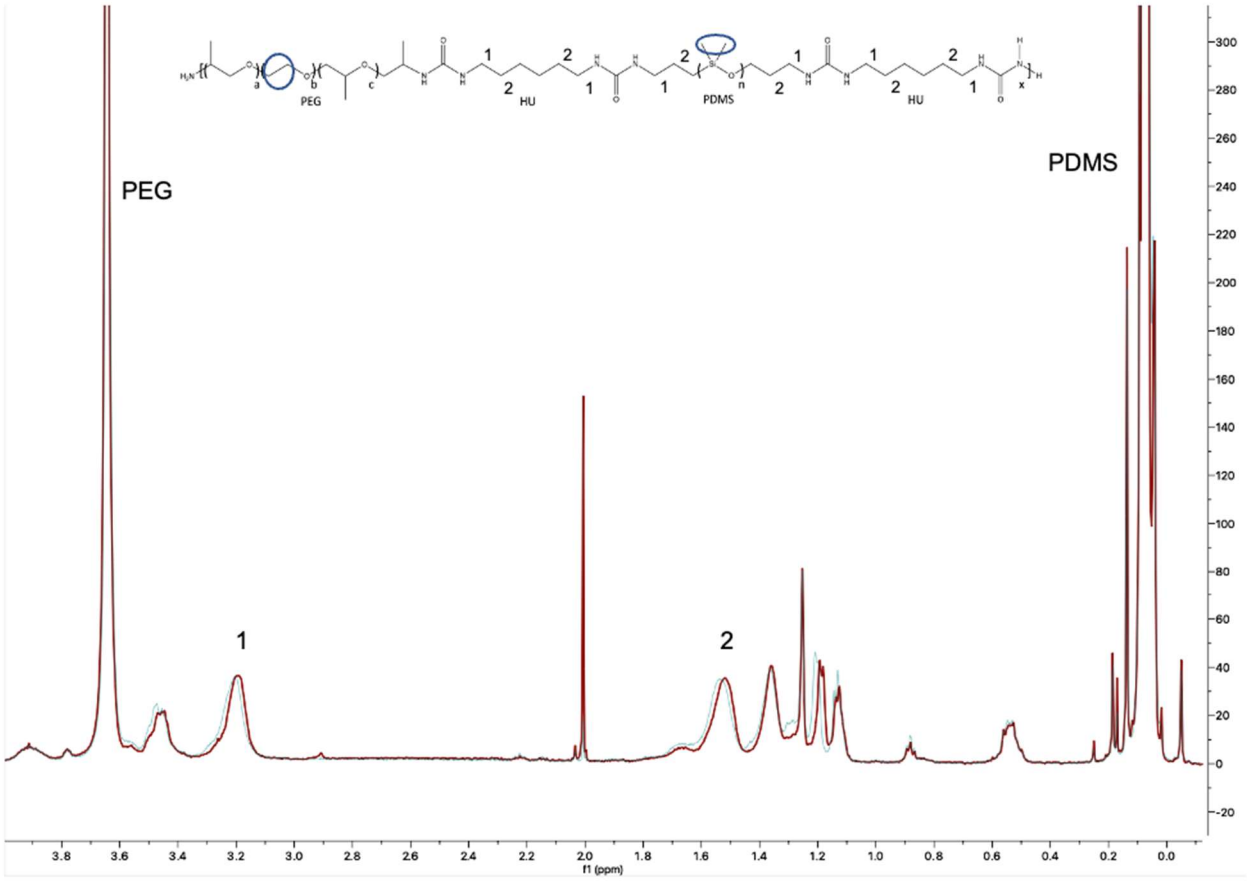

Figure S4. Superimposed NMR spectra of *R-PEG$_{0.9k}$-PDMS$_{3k}$-HU* and *P-PEG$_{0.9k}$-PDMS$_{3k}$-HU*.

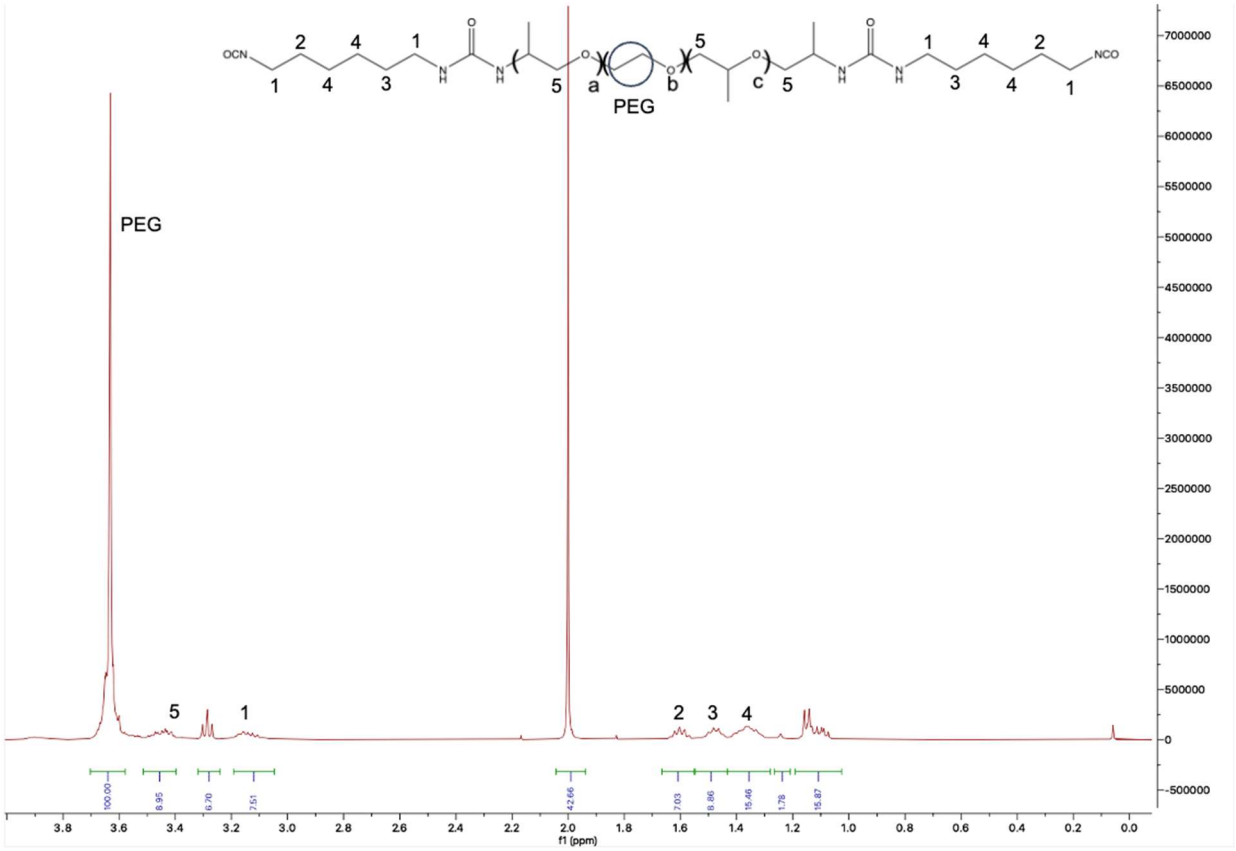

Figure S5. NMR spectra of diisocyanate-functionalized PEG intermediate (OCN-PEG-NCO).

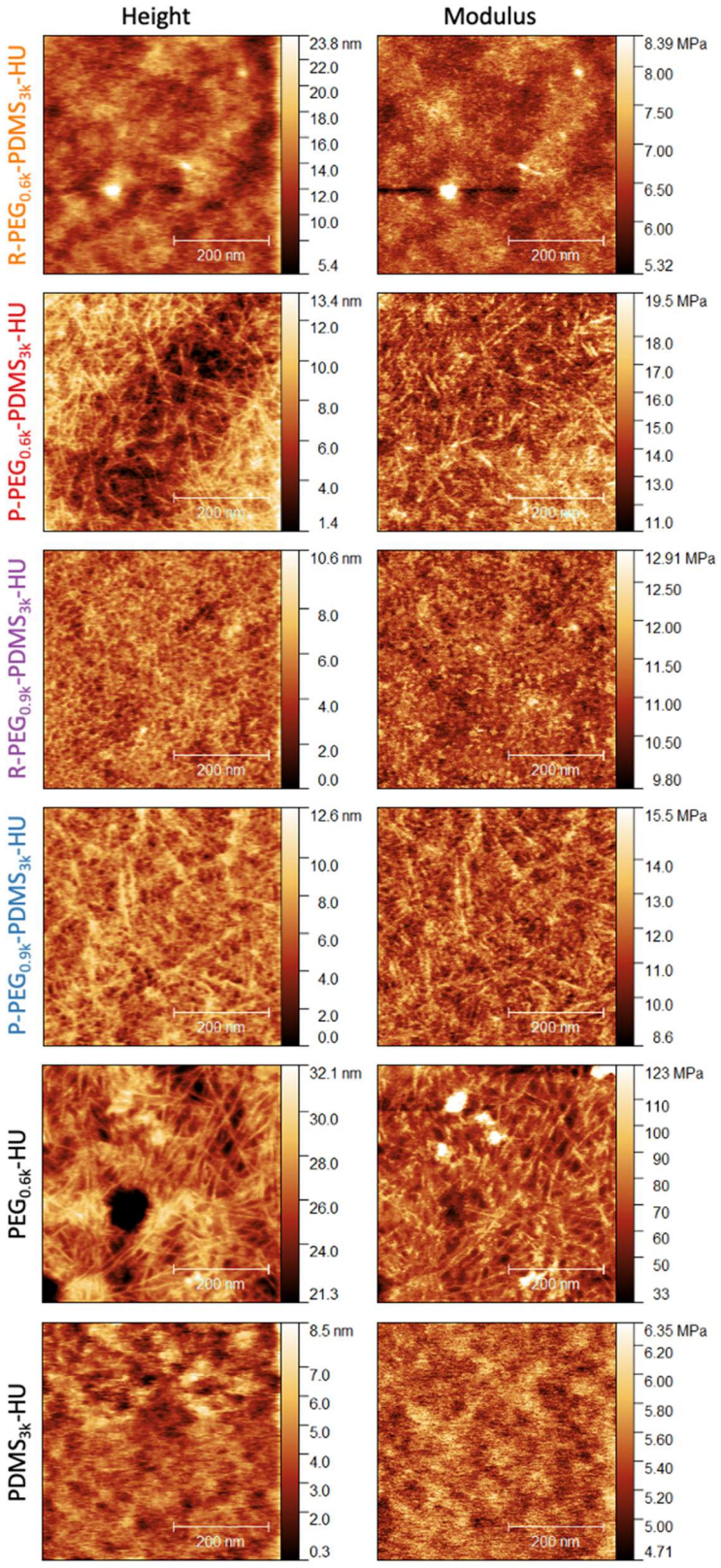

Figure S6. AFM-based quantitative nanomechanical imaging with height and stiffness profiles.

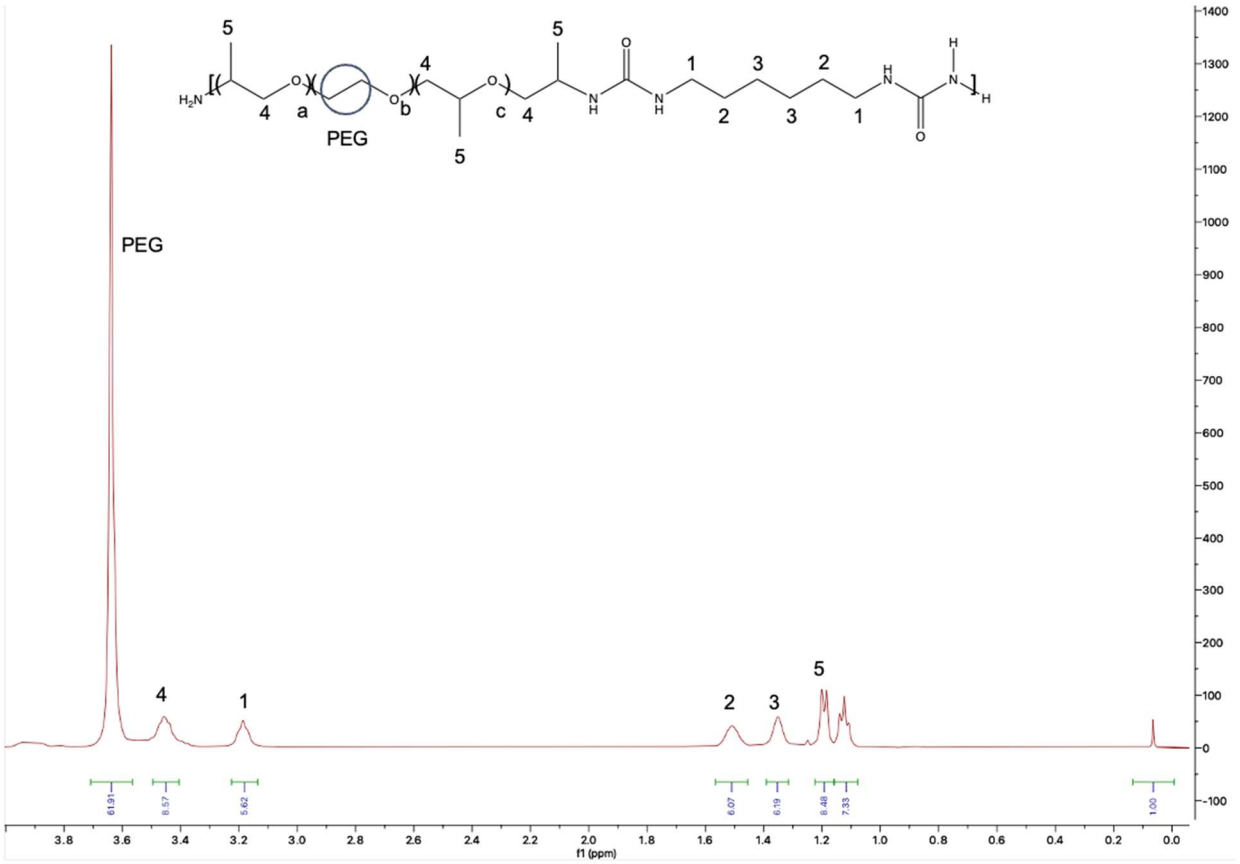

Figure S7. NMR spectra of *PEG$_{0.6k}$-HU*.

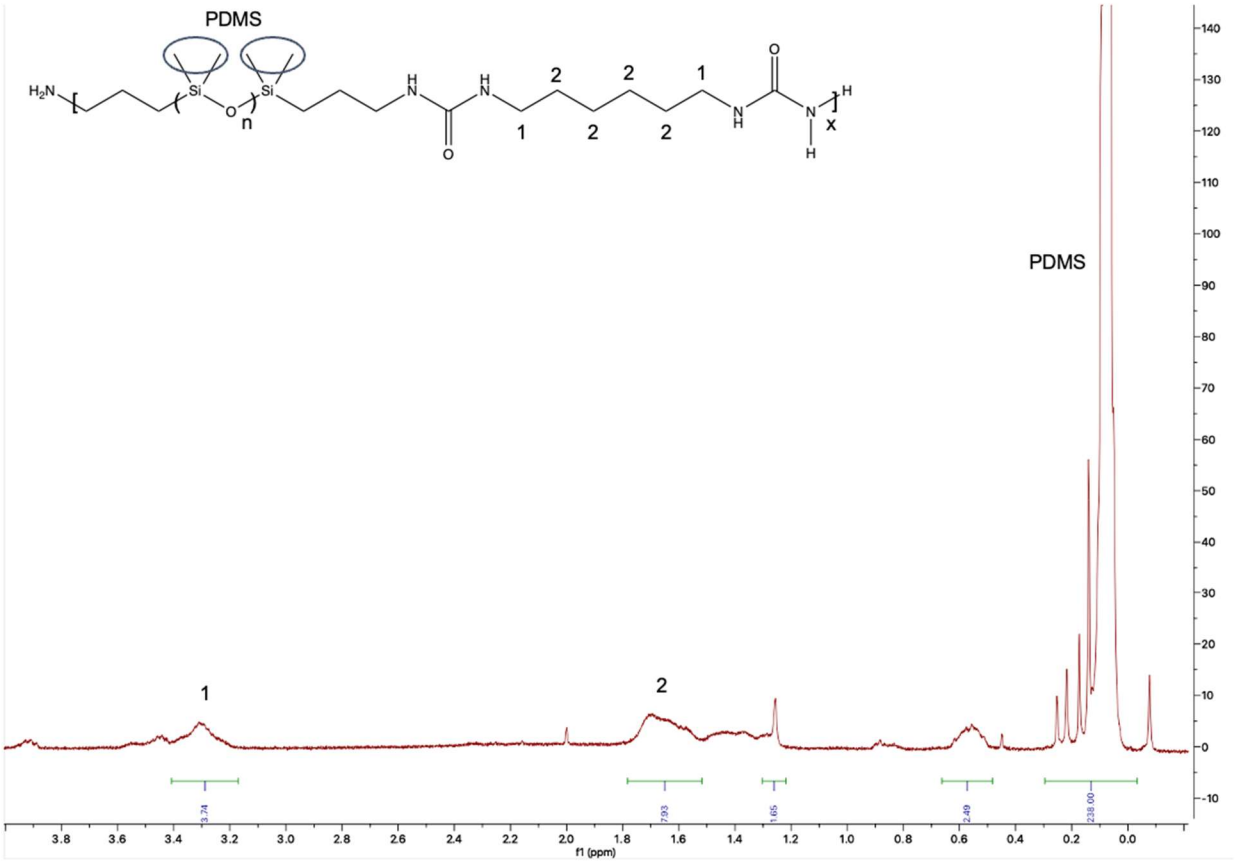

Figure S8. NMR spectra of *PDMS$_{3k}$-HU*.

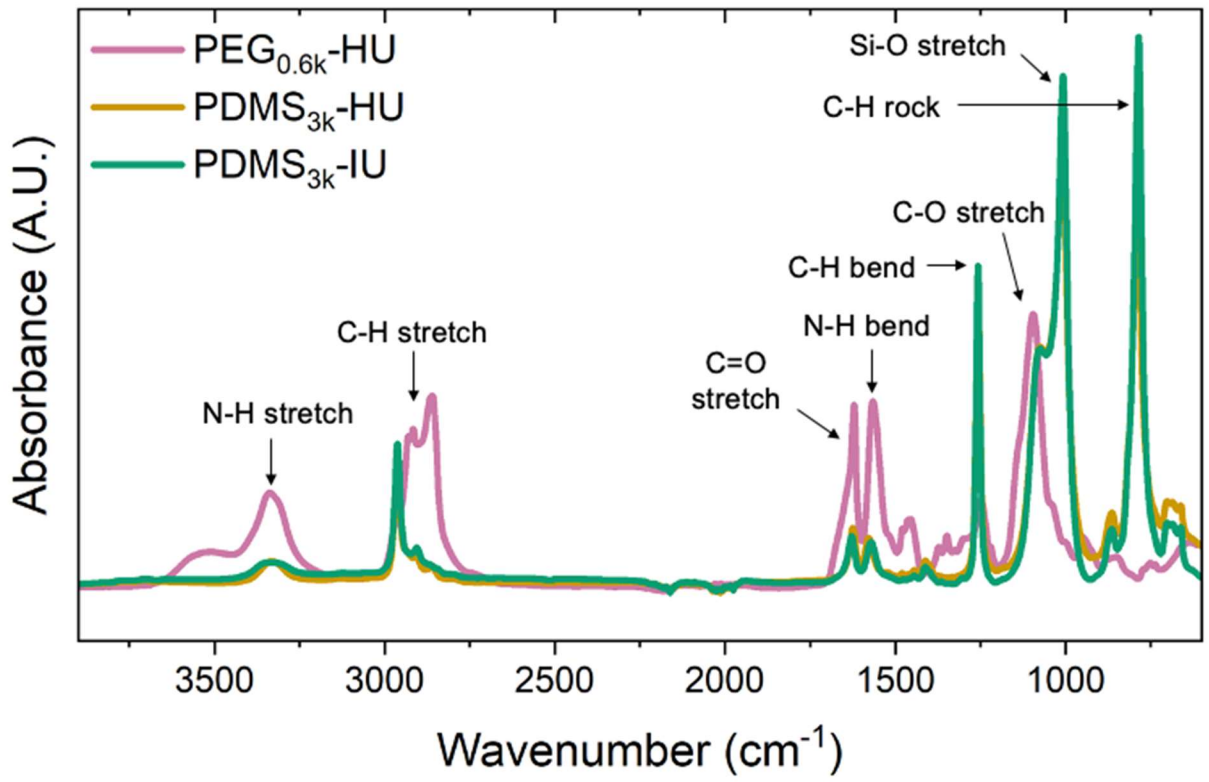

Figure S9. FTIR spectra for *PEG$_{0.6k}$-HU* (pink), *PDMS$_{3k}$-HU* (gold), and *PDMS$_{3k}$-IU* (green).

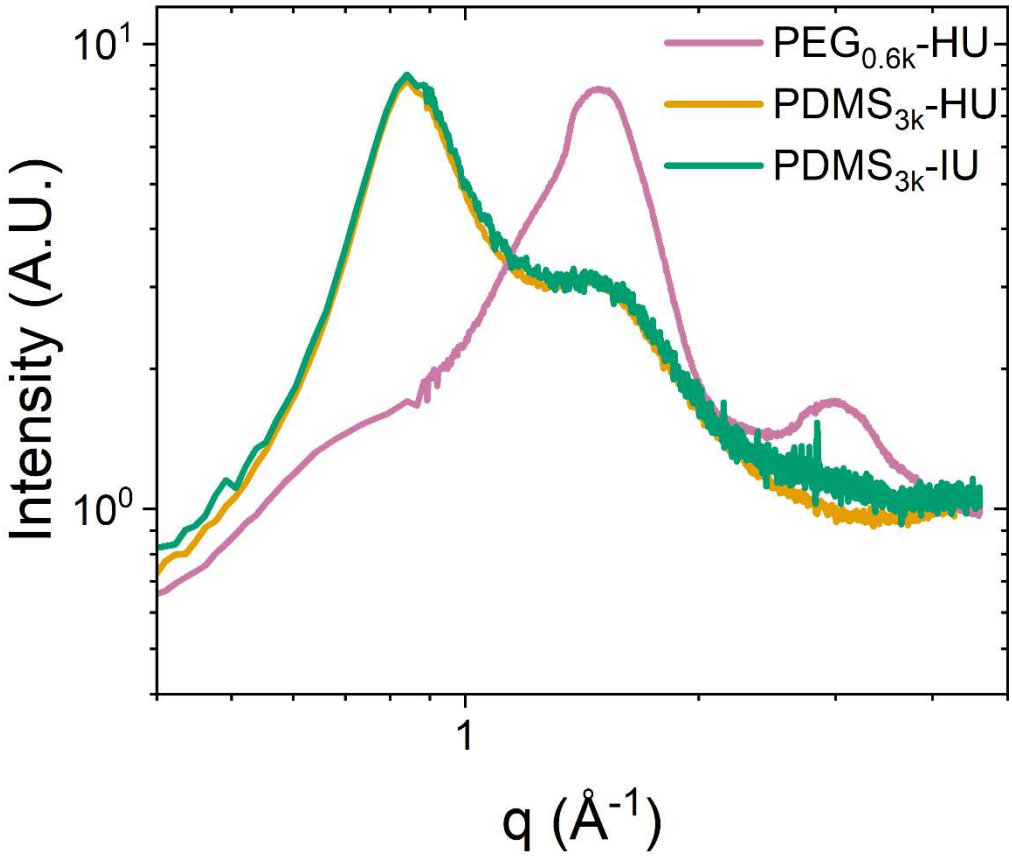

Figure S10. WAXS patterns for *PEG$_{0.6k}$-HU* (pink), *PDMS$_{3k}$-HU* (gold), and *PDMS$_{3k}$-IU* (green).

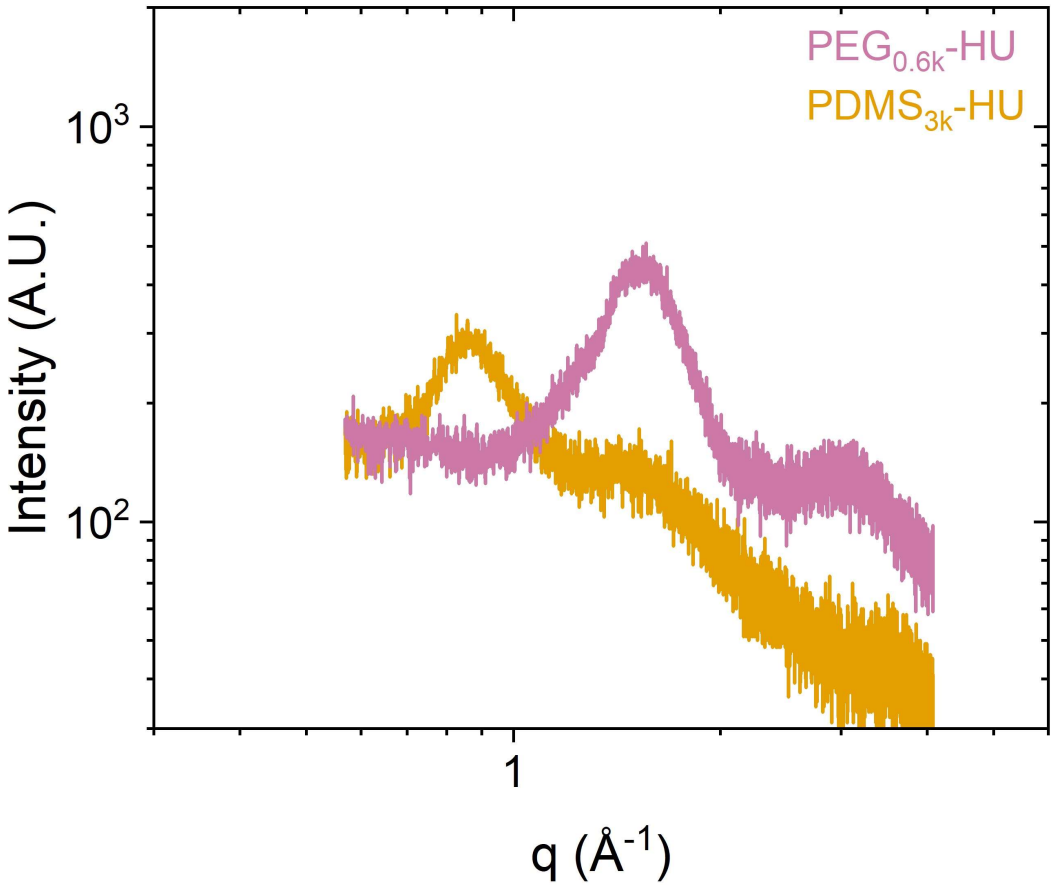

Figure S11. XRD pattern for *PEG$_{0.6k}$-HU* (pink) and *PDMS$_{3k}$-HU* (gold).

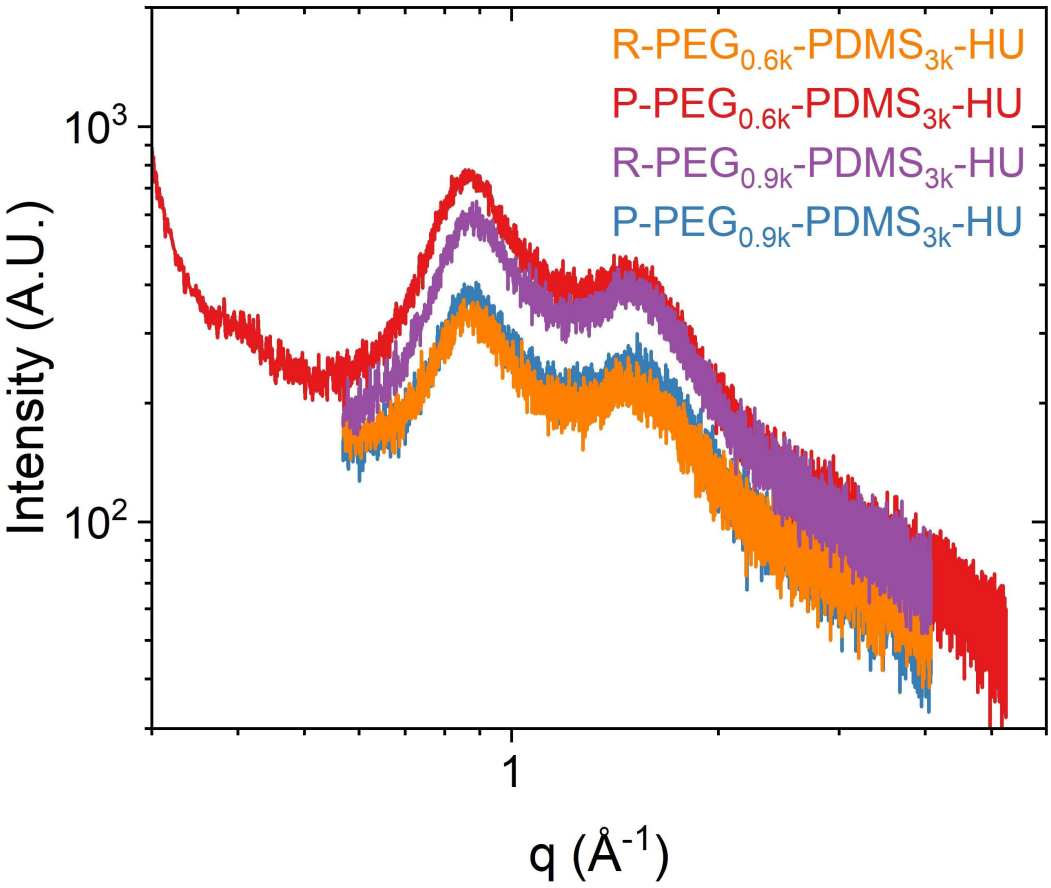

Figure S12. XRD patterns for *R-PEG$_{0.6k}$-PDMS$_{3k}$-HU* (orange), *P-PEG$_{0.6k}$-PDMS$_{3k}$-HU* (red), *R-PEG$_{0.9k}$-PDMS$_{3k}$-HU* (purple), and *P-PEG$_{0.9k}$-PDMS$_{3k}$-HU* (blue).

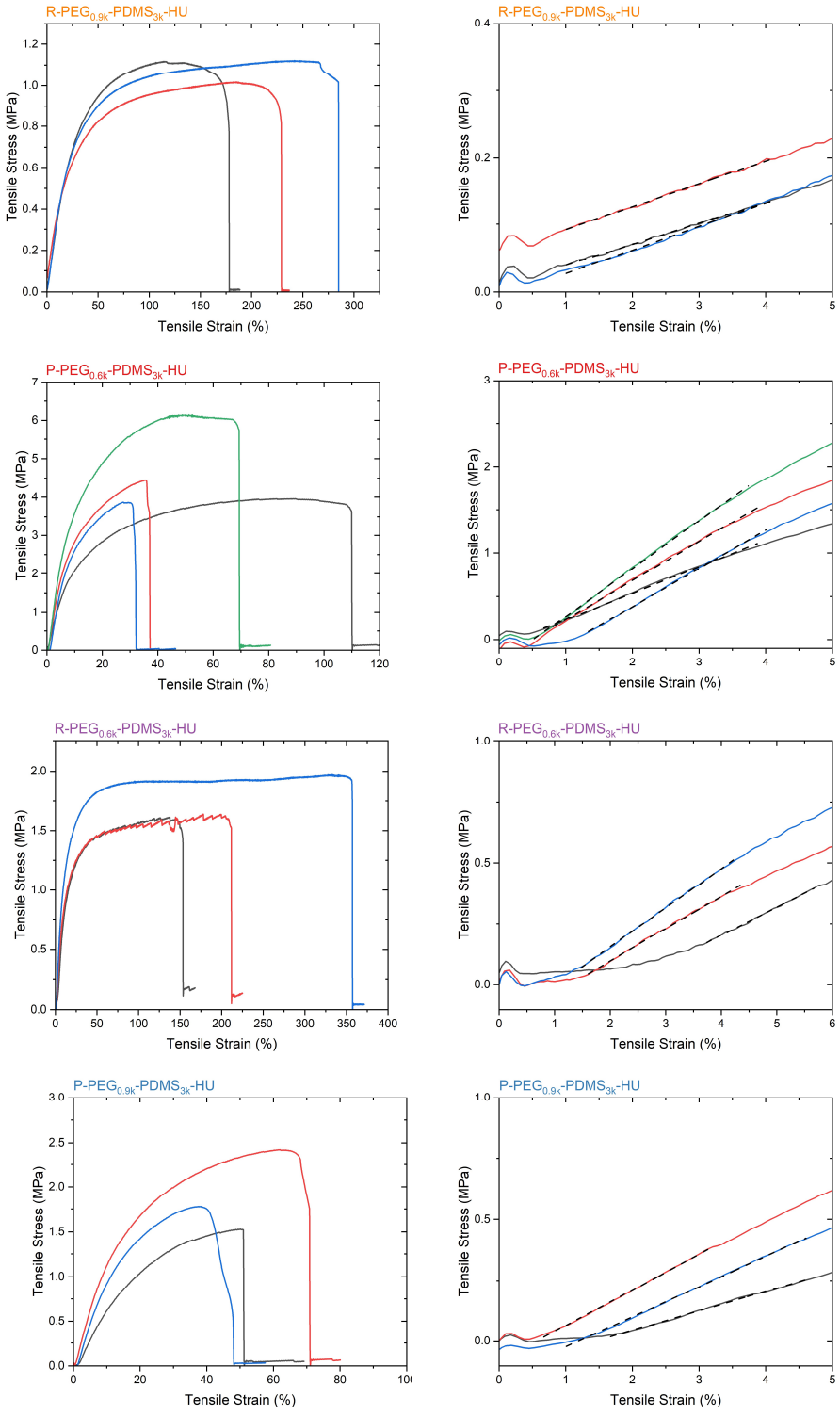

Figure S13. Stress-strain curves obtained from Instron tensile testing of n = 3 samples and the linear fit in the elastic regime to determine the Young's moduli.

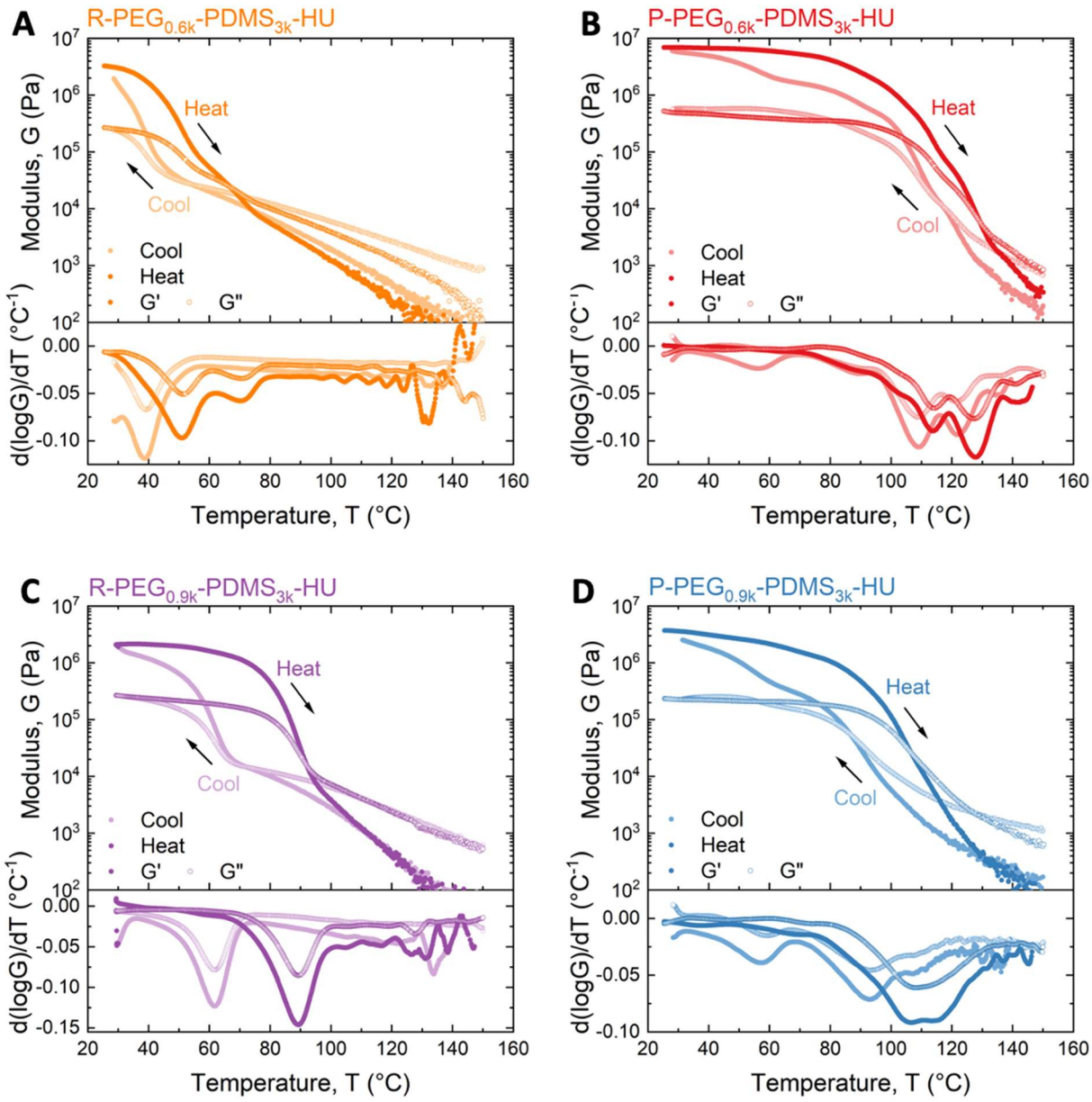

Figure S14. Rheological characterization and identification of thermal transitions. Storage (*G',* solid circles) and loss (*G",* open circles) shear moduli during heating (dark) and cooling (light) for (**A**) *R-PEG$_{0.6k}$-PDMS$_{3k}$-HU* (orange), (**B**) *P-PEG$_{0.6k}$-PDMS$_{3k}$-HU* (red), (**C**) *R-PEG$_{0.9k}$-PDMS$_{3k}$-HU* (purple), and (**D**) *P-PEG$_{0.9k}$-PDMS$_{3k}$-HU* (blue). The plots of the derivatives of the logarithm of the storage and loss shear moduli with respect to temperature have peaks that determine the temperatures of the thermal transitions upon heating and cooling.

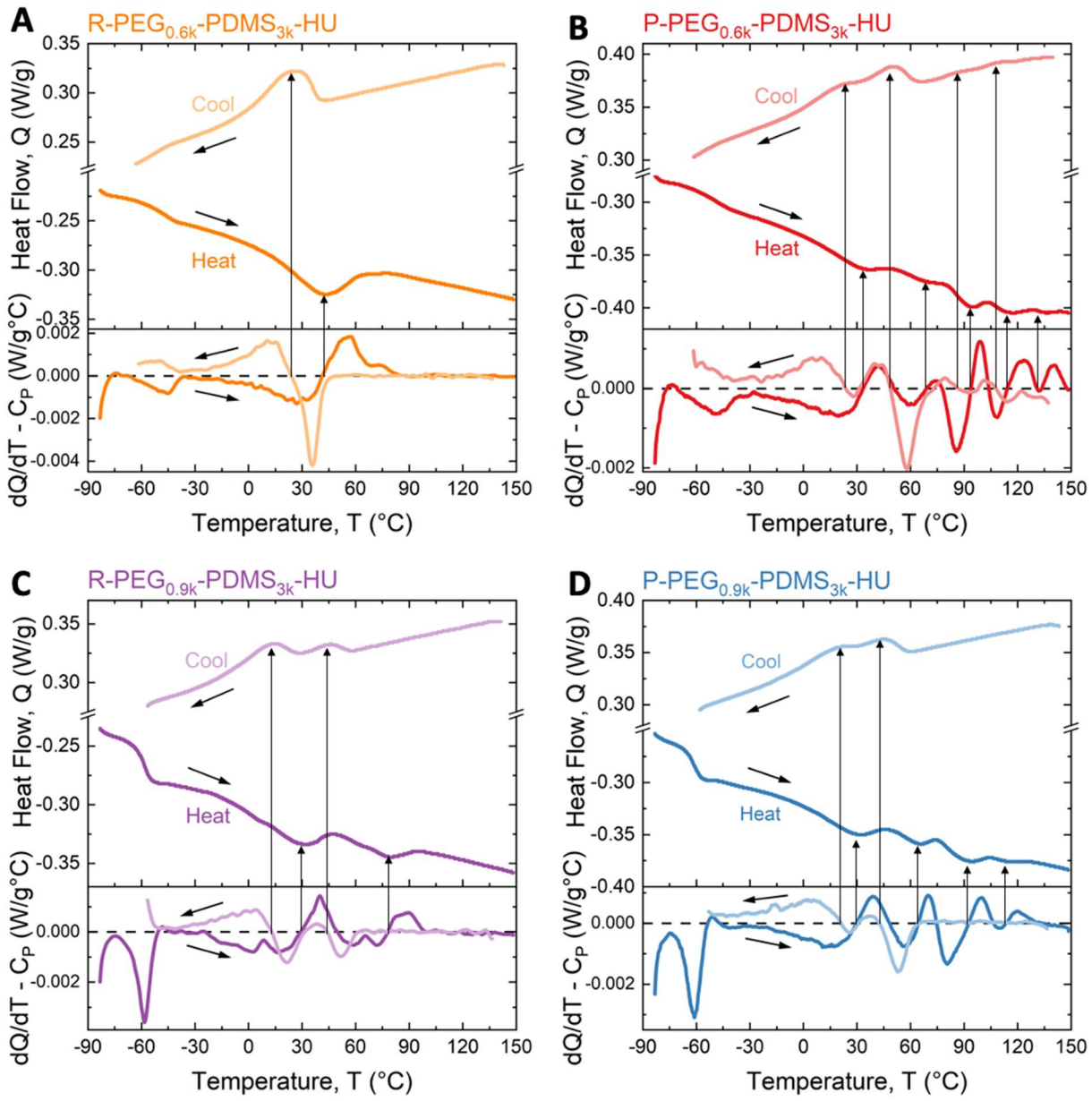

Figure S15. DSC curves on heating and cooling for (**A**) *R-PEG$_{0.6k}$-PDMS$_{3k}$-HU* (orange), (**B**) *P-PEG$_{0.6k}$-PDMS$_{3k}$-HU* (red), (**C**) *R-PEG$_{0.9k}$-PDMS$_{3k}$-HU* (purple), and (**D**) *P-PEG$_{0.9k}$-PDMS$_{3k}$-HU* (blue). The zeros of the derivative of the heat flow with respect to temperature subtracted by the heat capacity of the polymers is used to identify the peak transition temperatures.

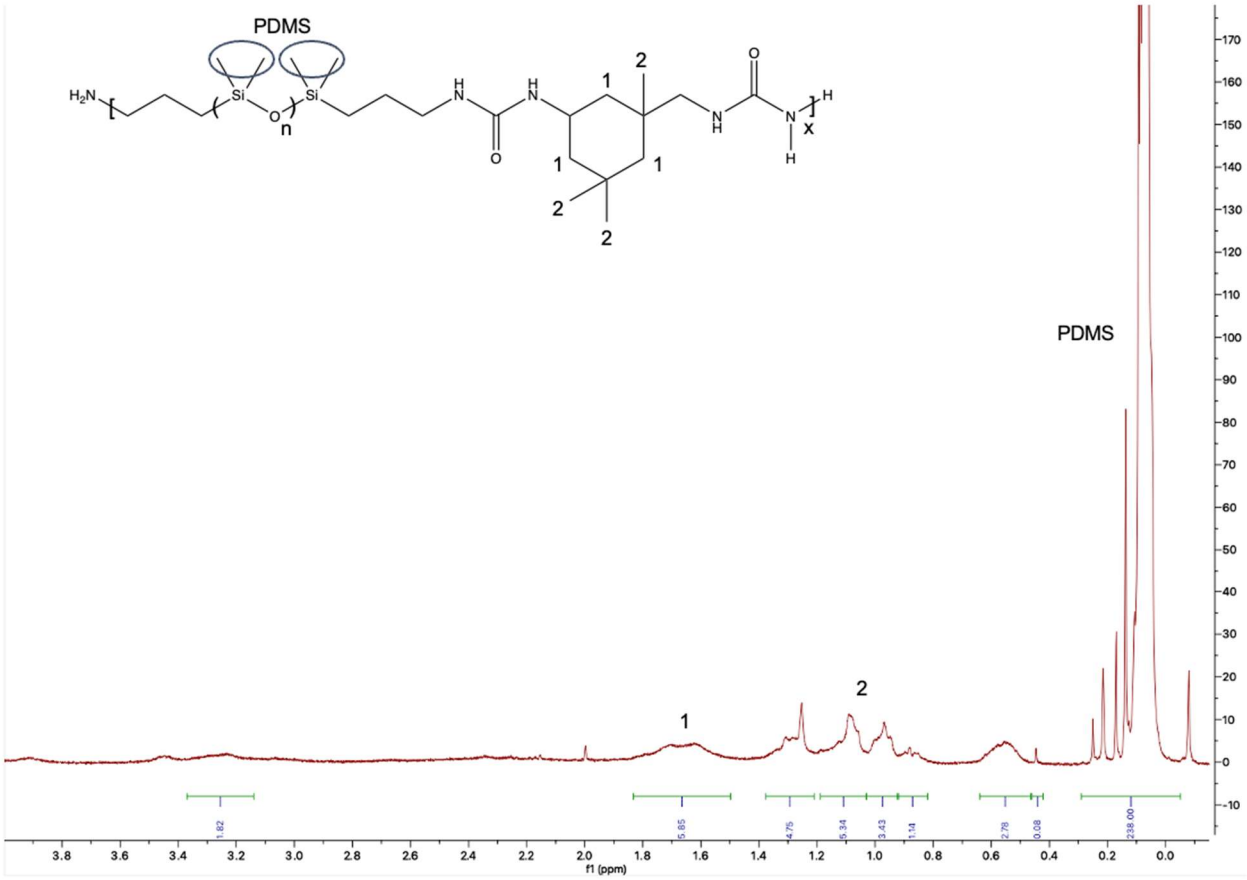

Figure S16. NMR spectra of *PDMS$_{3k}$-IU*.

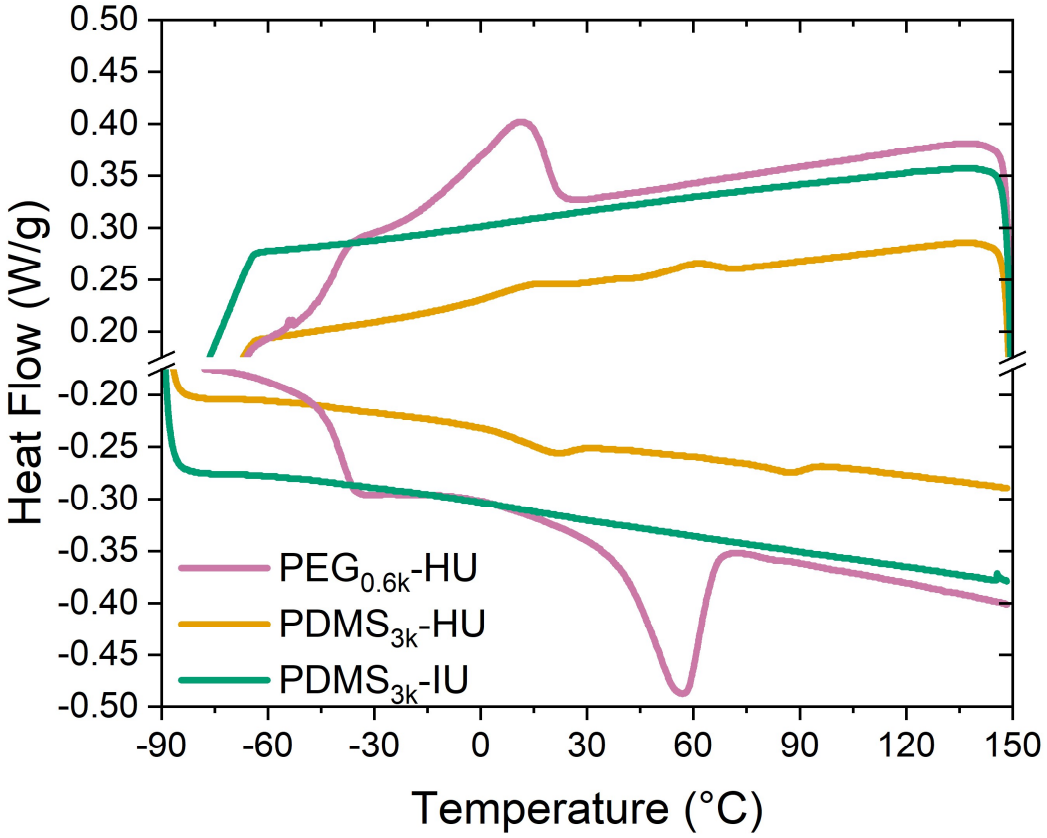

Figure S17. DSC curves for *PEG$_{0.6k}$-HU* (pink), *PDMS$_{3k}$-HU* (gold), and *PDMS$_{3k}$-IU* (green) upon heating and cooling. *PEG$_{0.6k}$-HU* undergoes one large thermal transition. *PDMS$_{3k}$-HU* undergoes two small transitions. *PDMS$_{3k}$-IU* undergoes no transitions.

Table S1. Weight fractions of PEG, PDMS, and HU components in the synthesized DBCPs.

Sample	PEG wt%	PDMS wt%	HU wt%
R-$PEG_{0.6k}$-$PDMS_{3k}$-HU	15	75	10
P-$PEG_{0.6k}$-$PDMS_{3k}$-HU	15	75	10
R-$PEG_{0.9k}$-$PDMS_{3k}$-HU	21	70	9
P-$PEG_{0.9k}$-$PDMS_{3k}$-HU	21	70	9
$PEG_{0.6k}$-HU	75	-	25
$PDMS_{3k}$-HU	-	94	6

Table S2. ^{1}H NMR integration.

Sample	# of H	PEG δ = 3.64	PDMS δ = 0.07	HU-1 δ = 3.19	HU-2 δ = 1.51	HU:PEG:PDMS
R-PEG$_{0.6k}$-PDMS$_{3k}$-HU	Expected	36	238	12	12	2:1:1
	Observed	36.5	238	10.7	10.3	1.78:1.01:1
P-PEG$_{0.6k}$-PDMS$_{3k}$-HU	Expected	36	238	12	12	2:1:1
	Observed	31.9	238	12.6	12.1	2.1:0.89:1
R-PEG$_{0.9k}$-PDMS$_{3k}$-HU	Expected	67	238	12	12	2:1:1
	Observed	64.6	238	11.7	11.4	1.95:0.96:1
P-PEG$_{0.9k}$-PDMS$_{3k}$-HU	Expected	67	238	12	12	2:1:1
	Observed	62.9	238	12.5	12.1	2.08:0.94:1
PEG$_{0.6k}$-HU	Expected	36	-	4	4	-
	Observed	44	-	4	4.3	-
PDMS$_{3k}$-HU	Expected	-	238	4	8	-
	Observed	-	238	3.7	7.9	-
Sample	# of H	PEG δ = 3.64	PDMS δ = 0.06	IU-1 δ = 1.66	IU-2 δ = 1.09	HU:PEG:PDMS
PDMS$_{3k}$-IU	Expected	-	238	6	9	-
	Observed	-	238	5.85	8.78	-

Table S3. Average modulus and roughness of polymer films by AFM-QNM.

Sample	Average Modulus (MPa)	RMS Roughness (MPa)
R-PEG$_{0.6k}$-PDMS$_{3k}$-HU	6.6	0.5
P-PEG$_{0.6k}$-PDMS$_{3k}$-HU	15	1
R-PEG$_{0.9k}$-PDMS$_{3k}$-HU	11.1	0.4
P-PEG$_{0.9k}$-PDMS$_{3k}$-HU	11.6	0.8
PEG$_{0.6k}$-HU	70	10
PDMS$_{3k}$-HU	5.5	0.2

Table S4. Small-angle X-ray scattering (SAXS) with the peak intensity at the scattering wavevector q, corresponding to an average domain spacing d.

Sample	q (Å^{-1})	d (nm)
R-PEG$_{0.6k}$-PDMS$_{3k}$-HU	0.053	12
P-PEG$_{0.6k}$-PDMS$_{3k}$-HU	0.068	9
R-PEG$_{0.9k}$-PDMS$_{3k}$-HU	0.046	14
P-PEG$_{0.9k}$-PDMS$_{3k}$-HU	0.062	10

Table S5. Instron tensile testing of n = 3 samples at a strain rate of 200%/min.

Sample	Young's Modulus *E* (MPa)	Tensile Strength (MPa)	Strain at Break (%)
R-PEG$_{0.6k}$-PDMS$_{3k}$-HU	13 ± 2	1.7 ± 0.2	200 ± 100
P-PEG$_{0.6k}$-PDMS$_{3k}$-HU	40 ± 10	5 ± 1	60 ± 40
R-PEG$_{0.9k}$-PDMS$_{3k}$-HU	3.3 ± 0.2	1.08 ± 0.06	230 ± 50
P-PEG$_{0.9k}$-PDMS$_{3k}$-HU	12 ± 3	1.9 ± 0.5	60 ± 10

Table S6. Rheological characterization with crossover temperatures upon cooling and heating.

Sample	Crossover Temperature on Cooling (℃)	Crossover Temperature on Heating (℃)	G' at 25 °C (MPa)	G'' at 25 °C (MPa)
R-PEG$_{0.6k}$-PDMS$_{3k}$-HU	54	66	3.3	0.27
P-PEG$_{0.6k}$-PDMS$_{3k}$-HU	117	129	6.9	0.52
R-PEG$_{0.9k}$-PDMS$_{3k}$-HU	73	92	2.1	0.27
P-PEG$_{0.9k}$-PDMS$_{3k}$-HU	87	107	3.7	0.23

Table S7. Rheological transitions obtained from d(logG')/dT.

	Transition Temperatures (°C)	
Sample	Heating	Cooling
R-PEG$_{0.6k}$-PDMS$_{3k}$-HU	51	39
	70	-
P-PEG$_{0.6k}$-PDMS$_{3k}$-HU	114	56
	128	90
	-	109
	-	122
R-PEG$_{0.9k}$-PDMS$_{3k}$-HU	89	62
P-PEG$_{0.9k}$-PDMS$_{3k}$-HU	110	57
	-	93

Table S8. Differential scanning calorimetry (DSC) cycling between -90 °C and 150 °C with glass transition temperatures, peak temperatures, and enthalpy changes. Total integration is the total enthalpy change integrated across all transitions from ~0 °C to ~140 °C.

		Heating		Cooling	
Sample	T_g (°C)	Peak Temperature (°C)	Enthalpy (J/g)	Peak Temperature (°C)	Enthalpy (J/g)
R-PEG$_{0.6k}$-PDMS$_{3k}$-HU	-50	41	7.9	24	6.5
P-PEG$_{0.6k}$-PDMS$_{3k}$-HU	-48	33	1.6	24	0.7
		69	0.2	49	1.2
		94	0.8	87	0.1
		114	0.5	108	0.1
		133	0.07	-	-
		Sum	3.17	Sum	2.1
		Total Integration	6.7	Total Integration	6.1
R-PEG$_{0.9k}$-PDMS$_{3k}$-HU	-59	29	3.3	13	2.2
		78	1.4	44	0.5
		Sum	4.7	Sum	2.7
		Total Integration	6.6	Total Integration	6.0
P-PEG$_{0.9k}$-PDMS$_{3k}$-HU	-62	30	2.0	21	0.9
		64	0.5	43	0.8
		93	1.1	-	-
		114	0.1	-	-
		Sum	3.7	Sum	1.7
		Total Integration	5.7	Total Integration	6.3
PEG$_{0.6k}$-HU	-40	57	16.3	10	12.6
PDMS$_{3k}$-HU	-	22	1.4	14	0.9
		87	0.8	62	0.7
		Sum	2.2	Sum	1.8
		Total Integration	4.1	Total Integration	3.4

Table S9. Ratio of total enthalpy change during heating to weight fraction of HU.

Sample	HU wt%	DSC Total Enthalpy (J/g)	Enthalpy:HU
R-PEG$_{0.6k}$-PDMS$_{3k}$-HU	10	7.9	0.79
P-PEG$_{0.6k}$-PDMS$_{3k}$-HU	10	6.7	0.67
R-PEG$_{0.9k}$-PDMS$_{3k}$-HU	9	6.6	0.73
P-PEG$_{0.9k}$-PDMS$_{3k}$-HU	9	5.7	0.63
PEG$_{0.6k}$-HU	25	16.3	0.65
PDMS$_{3k}$-HU	6	4.1	0.68

Table S10. Average ionic conductivity (σ) values for n = 2 samples upon heating and cooling taken at 30 °C, 70 °C, 110 °C, and 150 °C. Mass loading of LiTFSI salt in the polymers with $EO/Li^+ = 16$ except for $PDMS_{3k}$-HU.

Sample	LiTFSI (wt%)	σ at 30 °C (S/cm)	σ at 70 °C (S/cm)	σ at 110 °C (S/cm)	σ at 150 °C (S/cm)
R-$PEG_{0.6k}$-$PDMS_{3k}$-HU	4.5	2.2×10^{-9}	1.1×10^{-7}	1.6×10^{-6}	5.3×10^{-6}
P-$PEG_{0.6k}$-$PDMS_{3k}$-HU	4.5	6.4×10^{-7}	7.0×10^{-6}	4.1×10^{-5}	5.4×10^{-5}
R-$PEG_{0.9k}$-$PDMS_{3k}$-HU	7.8	1.9×10^{-9}	9.8×10^{-8}	1.3×10^{-6}	4.4×10^{-6}
P-$PEG_{0.9k}$-$PDMS_{3k}$-HU	7.8	9.0×10^{-9}	2.7×10^{-7}	3.7×10^{-6}	1.1×10^{-5}
$PEG_{0.6k}$-HU	20.8	3.2×10^{-6}	5.7×10^{-5}	2.5×10^{-4}	3.4×10^{-4}
$PDMS_{3k}$-HU	4.5	8.1×10^{-10}	4.1×10^{-8}	3.4×10^{-7}	1.2×10^{-6}

Supplementary References

1 P.-G. De Gennes, *Scaling concepts in polymer physics*, Cornell University Press, 1979.